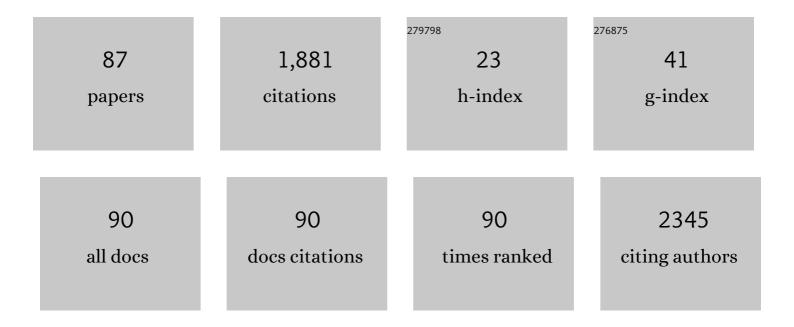
Wilfried Wunderlich

List of Publications by Year in descending order

Source: https://exaly.com/author-pdf/9266415/publications.pdf Version: 2024-02-01



#	Article	IF	CITATIONS
1	Ethyl benzene oxidation under aerobic conditions using cobalt oxide imbedded in nitrogen-doped carbon fiber felt wrapped by spiral TiO2-SiO2. Applied Catalysis A: General, 2022, 630, 118456.	4.3	5
2	In situ generated Ligand-Free gold nanoparticles in polyvinylpyrrolidone solution assisted laser in liquid method for green oxidation of cyclohexane to adipic acid with high yield. Applied Surface Science, 2022, 581, 152388.	6.1	2
3	Efficient photocatalyst for the degradation of cationic and anionic dyes prepared via modification of carbonized mesoporous TiO2 by encapsulation of carbon dots. Materials Research Bulletin, 2022, 155, 111963.	5.2	8
4	Chat Bot Concept for a Social Pain Reliever. , 2021, , .		1
5	Au-Pd nanoparticles enfolded in coil-like TiO2 immobilized on carbon fibers felt as recyclable nanocatalyst for benzene oxidation under mild conditions. Applied Surface Science, 2020, 506, 144644.	6.1	16
6	Preparation and Photocatalytic Properties of CdS and ZnS Nanomaterials Derived from Metal Xanthate. Materials, 2019, 12, 3313.	2.9	24
7	Au-Pd@g-C ₃ N ₄ as an Efficient Photocatalyst for Visible-Light Oxidation of Benzene to Phenol: Experimental and Mechanistic Study. Journal of Physical Chemistry C, 2018, 122, 27477-27485.	3.1	58
8	Laser-Ablated ZnO Nanoparticles and Their Photocatalytic Activity toward Organic Pollutants. Materials, 2018, 11, 1127.	2.9	72
9	Processing and Thermoelectric Properties of New Si-/ Se-/ Sn-Based Intermetallics. Materials Science Forum, 2016, 879, 2131-2137.	0.3	1
10	Parameters for Improving Titania as Photo Catalysis Material. Materials Today: Proceedings, 2016, 3, 662-666.	1.8	0
11	Pd Loaded TiO2 Nanotubes for the Effective Catalytic Reduction of p-Nitrophenol. Catalysis Letters, 2016, 146, 474-482.	2.6	28
12	Energy Harvesting under Large Temperature Gradient – Comparison of Silicides, Half-Heusler Alloys and Ceramics. Energy Harvesting and Systems, 2015, 2, 37-46.	2.7	2
13	An aqueous method for the controlled manganese (Mn ²⁺) substitution in superparamagnetic iron oxide nanoparticles for contrast enhancement in MRI. Physical Chemistry Chemical Physics, 2015, 17, 4609-4619.	2.8	27
14	Thermoelectric Properties of Mg2Si Produced by New Chemical Route and SPS. Inorganics, 2014, 2, 351-362.	2.7	12
15	SPS-sintered NaTaO3–Fe2O3 composite exhibits enhanced Seebeck coefficient and electric current. Materials for Renewable and Sustainable Energy, 2014, 3, 1.	3.6	5
16	Electronic Band-Structure Calculations of Ba8Me x Si46-x Clathrates with MeÂ=ÂMg, Pd, Ni, Au, Ag, Cu, Zn, Al, Sn. Journal of Electronic Materials, 2014, 43, 1527-1532.	2.2	8
17	Improvement of thermoelectric TiZrNiSn thin films by contact layers. , 2014, , .		0
18	The Atomistic Structure of Metal/Ceramic Interfaces Is the Key Issue for Developing Better Properties. Metals, 2014, 4, 410-427.	2.3	37

#	Article	IF	CITATIONS
19	Enhanced Microwave Resonance Properties of Pseudo-Tungsten-Bronze Ba _{6-3x} R _{8+2x} Ti ₁₈ O ₅₄ (R = Rare Earth) Solid Solutions Explained by Electron–Phonon Interaction. Japanese Journal of Applied Physics, 2013, 52, 09KH04.	1.5	5
20	Magnetron sputtering of (TiZr)NiSn thin films on different substrates for thermoelectric applications. Journal of Physics: Conference Series, 2012, 379, 012005.	0.4	4
21	Synthesis and Characterization of Iron Oxide Embedded Hydroxyapatite Bioceramics. Journal of the American Ceramic Society, 2012, 95, 2695-2699.	3.8	63
22	The Difference Between Thermo- and Pyroelectric Co-Based Rare-Earth (Nd, Y, Gd, Ce) Oxide Composites Measured Using a High Temperature Gradient. Journal of Electronic Materials, 2011, 40, 127-133.	2.2	4
23	Large Closed-Circuit Seebeck Current in Quaternary (Ti,Zr)NiSn Heusler Alloys. Journal of Electronic Materials, 2011, 40, 583-588.	2.2	9
24	Highâ€ S urfaceâ€Area Alumina–Silica Nanocatalysts Prepared by a Hybrid Sol–Gel Route Using a Boehmite Precursor. Journal of the American Ceramic Society, 2010, 93, 4047-4052.	3.8	12
25	Critical Nuclei Size, Initial Particle Size and Packing Effect on the Phase Stability of Sol-Peptization-Gel-Derived Nanostructured Titania. Langmuir, 2010, 26, 4567-4571.	3.5	20
26	Mesoporous gadolinium doped titania photocatalyst through an aqueous sol–gel method. Journal of Alloys and Compounds, 2010, 505, 194-200.	5.5	36
27	Ceramic Materials. , 2010, , .		7
28	New aspects about reduced LCF-life time of spherical ductile cast iron due to dynamic strain aging at intermediate temperatures. Journal of Nuclear Materials, 2009, 389, 137-141.	2.7	2
29	High surface area sol–gel alumina–titania nanocatalyst. Journal of Sol-Gel Science and Technology, 2009, 52, 88-96.	2.4	11
30	Thermally stable nanophase anatase titania with mesoporous texture by pseudo-inorganic templating. Microporous and Mesoporous Materials, 2009, 120, 467-471.	4.4	0
31	Enhanced effective mass in doped SrTiO3 and related perovskites. Physica B: Condensed Matter, 2009, 404, 2202-2212.	2.7	144
32	NaTaO3 composite ceramics – A new thermoelectric material for energy generation. Journal of Nuclear Materials, 2009, 389, 57-61.	2.7	26
33	Magnetostriction properties of FePd thin films: Dependence on microstructure. Journal of Alloys and Compounds, 2009, 475, 339-342.	5.5	9
34	Effect of Dynamic Strain Aging on Isothermal (473 K) Low Cycle Fatigue of Ferritic Ductile Cast Iron. Materials Transactions, 2009, 50, 1935-1940.	1.2	4
35	Al2O3 @ TiO2—A simple sol–gel strategy to the synthesis of low temperature sintered alumina–aluminium titanate composites through a core–shell approach. Journal of Solid State Chemistry, 2008, 181, 2748-2754.	2.9	23
36	Reduced band-gap due to phonons in SrTiO3 analyzed by ab initio calculations. Solid-State Electronics, 2008, 52, 1082-1087.	1.4	8

WILFRIED WUNDERLICH

#	Article	IF	CITATIONS
37	Screening and Fabrication of Half-Heusler Phases for Thermoelectric Applications. Materials Research Society Symposia Proceedings, 2008, 1128, 11001.	0.1	3
38	Growth model for plasma-CVD growth of carbon nano-tubes on Ni-sheets. Diamond and Related Materials, 2007, 16, 369-378.	3.9	29
39	Effect of tantalum addition on anatase phase stability and photoactivity of aqueous sol–gel derived mesoporous titania. Journal of Molecular Catalysis A, 2007, 276, 41-46.	4.8	48
40	Enhanced photoactivity and anatase thermal stability of silica–alumina mixed oxide additives on sol–gel nanocrystalline titania. Materials Letters, 2007, 61, 1751-1755.	2.6	27
41	Enhanced photoactivity of neodymium doped mesoporous titania synthesized through aqueous sol–gel method. Journal of Sol-Gel Science and Technology, 2007, 43, 283-290.	2.4	21
42	Nitrogenation of FePt nanoparticles. Journal of Nanoparticle Research, 2007, 9, 507-511.	1.9	0
43	Dielectric constant dependence on atomic substitution of Y2BaCuO5 clarified by ab initio calculations. Journal of the European Ceramic Society, 2006, 26, 1869-1872.	5.7	4
44	Structural aspects and porosity features of nano-size high surface area alumina–silica mixed oxide catalyst generated through hybrid sol–gel route. Materials Chemistry and Physics, 2006, 95, 56-61.	4.0	35
45	Thermodynamical Calculations and Experimental Confirmation about the Mg-Al-Spinel Reaction Path in the Sol-Gel-Process. Key Engineering Materials, 2006, 317-318, 135-138.	0.4	1
46	Effective Electron Mass of ordered AgPbmSbTe2+m clarified by ab-initio calculations. , 2006, , .		0
47	Development of high-temperature thermoelectric materials based on SrTiO ₃ -layered perovskites. International Journal of Materials Research, 2006, 97, 657-662.	0.8	11
48	Nanocomposites—a new material design concept. Science and Technology of Advanced Materials, 2005, 6, 2-10.	6.1	177
49	Fabrication and characterization of anatase/rutile–TiO2thin films by magnetron sputtering: a review. Science and Technology of Advanced Materials, 2005, 6, 11-17.	6.1	95
50	An aqueous sol–gel route to synthesize nanosized lanthana-doped titania having an increased anatase phase stability for photocatalytic application. Materials Chemistry and Physics, 2005, 90, 123-127.	4.0	86
51	Effective mass and thermoelectric properties of SrTiO/sub 3/-based natural superlattices evaluated by ab-initio calculations. , 2005, , .		1
52	AB-INITIO CALCULATIONS OF THE OPTICAL BAND GAP OF TiO2 THIN FILMS. International Journal of Nanoscience, 2004, 03, 439-445.	0.7	37
53	TEM characterization of sol-gel-processed alumina–silica and alumina–titania nano-hybrid oxide catalysts. Journal of the European Ceramic Society, 2004, 24, 313-317.	5.7	21
54	Impedance spectral studies of sol-gel alumina-silver nanocomposites. Acta Materialia, 2003, 51, 3511-3519.	7.9	13

WILFRIED WUNDERLICH

#	Article	IF	CITATIONS
55	Size Effect for Lead Zirconium Titanate Nanopowders with Pb(Zr0.3Ti0.7)O3Composition. Japanese Journal of Applied Physics, 2002, 41, 6985-6988.	1.5	17
56	Molecular dynamics — simulations of the fracture toughness of sapphire. Materials & Design, 2001, 22, 53-59.	5.1	35
57	Formation of stacking faults from misfit dislocations at the BaTiO3/SrTiO3 interface simulated by molecular dynamics. Materials Science & Engineering A: Structural Materials: Properties, Microstructure and Processing, 2001, 309-310, 148-151.	5.6	7
58	Molecular dynamics calculations about misfit dislocations at the BaTiO3/SrTiO3-interface. Thin Solid Films, 2000, 375, 9-14.	1.8	22
59	Molecular Dynamics-Simulations of the Fracture Toughness of Sapphire. Progress of Theoretical Physics Supplement, 2000, 138, 156-158.	0.1	2
60	Atomic Structure of Symmetrical Tilt Grain Boundaries in Zinc Oxide with High Coincidence. Physica Status Solidi A, 1998, 170, 99-111.	1.7	11
61	Molecular Dynamics Simulation of Alumina Interfaces in Order to Design Advanced Materials. Key Engineering Materials, 1998, 161-163, 449-452.	0.4	1
62	Optical and synchrotron radiation white-beam topographic investigations during the high-temperature phase transitions of KLiSO4. Ferroelectrics, 1997, 191, 171-177.	0.6	37
63	Interfacial chemical stability during diffusion bonding of Al2O3-fibres with Ni3Al- and NiAl-matrices. Acta Materialia, 1996, 44, 2383-2396.	7.9	20
64	Theoretical Considerations about Grain Boundary Migration in FCC Metals. Materials Science Forum, 1996, 207-209, 141-144.	0.3	0
65	In-Situ Observations of Grain Boundary Migration. Materials Science Forum, 1996, 204-206, 99-108.	0.3	12
66	Interfacial Chemical Stability During Diffusion Bonding of Al ₂ 0 ₃ Fibres with Ni ₃ Al and NiAl Matrices. Canadian Metallurgical Quarterly, 1995, 34, 231-236.	1.2	2
67	Interfacial chemical stability during diffusion bonding of Al2O3 fibres with Ni3Al and NiAl matrices. Canadian Metallurgical Quarterly, 1995, 34, 231-236.	1.2	2
68	Existence of enhanced solid state diffusion during mechanical alloying of Si and Ge. Applied Physics Letters, 1995, 66, 1903-1905.	3.3	11
69	A microscopic model for the mechanical alloying of silicon and germanium. Scripta Metallurgica Et Materialia, 1995, 33, 407-413.	1.0	7
70	Microstructure of mechanical alloyed Si76 Ge23.95 P0.05. Scripta Materialia, 1995, 6, 441-444.	0.5	7
71	On a high-purity Ge EDS detector II. Ice layer formation and optimization of detector design. Ultramicroscopy, 1993, 50, 219-227.	1.9	2
72	On a high-purity Ge EDS detector III. The reliable acquisition of EDS spectra. Ultramicroscopy, 1993, 50, 229-235.	1.9	1

#	Article	IF	CITATIONS
73	On the quantitative EDS analysis of low carbon concentrations in analytical TEM. Ultramicroscopy, 1993, 49, 220-224.	1.9	11
74	Arrangement of misfit dislocations at Ti3Al/TiAl phase boundaries. Materials Science & Engineering A: Structural Materials: Properties, Microstructure and Processing, 1993, 164, 421-427.	5.6	10
75	A New Discussion of the Interaction Energy in the Solid Solution Hardening of B.C.C. Iron Alloys. Physica Status Solidi A, 1993, 135, 391-403.	1.7	19
76	Mobile dislocations at the α2/γ phase boundaries in intermetallic TiAl/Ti3Al-alloys. Acta Metallurgica Et Materialia, 1993, 41, 1791-1799.	1.8	44
77	Formation of L12ordered precipitates at room temperature and their effect on the mechanical properties in Al-Li alloys. Philosophical Magazine A: Physics of Condensed Matter, Structure, Defects and Mechanical Properties, 1993, 67, 99-107.	0.6	15
78	Tem-studies of grain boundaries in cyclically deformed Alî—,Znî—,Mg-bicrystals. Acta Metallurgica Et Materialia, 1992, 40, 2123-2129.	1.8	5
79	Strength properties and enhanced plasticity of intermetallic Tiî—,Alî—,(CrSi) alloys. Materials Science & Engineering A: Structural Materials: Properties, Microstructure and Processing, 1992, 152, 166-172.	5.6	21
80	Effect on global and regional left ventricular functions by percutaneous transluminal coronary angioplasty in the chronic stage after myocardial infarction. American Journal of Cardiology, 1992, 69, 997-1002.	1.6	23
81	HREM-studies of the microstructure of nanocrystalline palladium. Scripta Metallurgica Et Materialia, 1990, 24, 403-408.	1.0	197
82	INFLUENCE OF HYDROGEN ON THE INTERFACE STRUCTURE AND PROPERTIES OF FATIGUED Al-Zn-Mg-BICRYSTALS. Journal De Physique Colloque, 1990, 51, C1-709-C1-714.	0.2	0
83	Fractal Aspects of the Martensitic Transformation in Zirconia. , 1989, , .		Ο
84	TEM studies on phases and phase stabilities of zirconia ceramics. Physica B: Physics of Condensed Matter & C: Atomic, Molecular and Plasma Physics, Optics, 1988, 150, 86-98.	0.9	20
85	High Resolution Electron Microscopy of Grain Boundaries in Sintered High-Tc Superconductor YBa2Cu3O7-x. Materials Research Society Symposia Proceedings, 1988, 122, 515.	0.1	1
86	Interaction of Palladium Nano-Crystals with Hydrogen During PECVD Growth of Carbon Nanotubes. Advances in Solid State Physics, 0, , 171-180.	0.8	11
87	Correlation of Segregation Energies of Ni and Fe with Mendeleev Number. Materials Science Forum, 0, 1016–1642-1646	0.3	Ο